E-9830

Laser Light Scattering, From an Advanced Technology Development Program to Experiments in a Reduced Gravity Environment

W. V. Meyer[†], W. W. Tscharnuter[‡], A. D. MacGregor[f], H. Dautet[f], P. Deschamps[f], F. Boucher[f], J. Zhu[§], P. Tin[†], R. B. Rogers[†], R. R. Ansari[†]

[†]William V. Meyer - NASA Lewis / OAI
Padetha Tin - NASA Lewis / CWRU
Richard B. Rogers - NASA Lewis
Rafat R. Ansari - NASA Lewis / CWRU
M.S. 105-1
21000 Brookpark Road
Cleveland, OH 44135-3191
Tel.: (216) 433-5011

[‡]Walther W. Tscharnuter
Brookhaven Instruments Corporation
750 Blue Point Road
Holtsville, NY 11742-1832

[f]Andrew D. MacGregor
Henri Dautet
Pierre Deschamps
François Boucher
EG&G Optoelectronics Canada
P.O. Box 900
22001 Dumberry Road
Vaudreuil, Québec J7V 8P7, Canada

[§]Jixiang Zhu
Princeton University
Department of Chemical Engineering
The Engineering Quadrangle, Olden Street
Princeton, NJ 08544

Abstract

We describe recent advancements in laser light scattering hardware including intelligent single card correlators, active quench/active reset avalanche photodiodes, laser diodes, and fiber optics which were used by or developed for a NASA Advanced Technology Development program. We then preview a space shuttle experiment which will employ aspects of these hardware developments.

Introduction

A new generation of hardware has been developed for NASA's Advanced Technology Development (ATD) program in laser light scattering (LLS).[1,2] These developments are coupled with both ground-based and flight proposals which have been accepted through the peer-reviewed NASA Research Announcement (NRA) selection process. This combination is culminating in a number of laser light scattering flight hardware instruments. We will discuss the primary modules used in the laser light scattering program and will single out for review a space shuttle LLS experiment which uses many of these components.

International Symposium on Space Optics, April 18-22, 1994, Garmisch-Partenkirchen, FRG, EOS/SPIE Joint Venture, paper 2210-21.

The instrument components to be presented include (a) an intelligent single card correlator capable of functioning in a simultaneous array with independent processors, (b) compact, highly efficient active quench/active reset avalanche photodiodes (APDs) which display many enhanced capabilities, (c) compact, inexpensive laser diodes, and (d) fiber optic source and detection paths that minimize alignment problems, and fiber optic sensors capable of replacing traditional optical components which when terminated differently are capable of avoiding many of the multiple scattering problems encountered at high concentrations. These building blocks have given us a flexible set of instrument components capable of being customized for the needs of particular experiments without forcing us to make design compromises. The Colloidal Disorder-Order Transition (CDOT) glovebox experiment (e) is an example of how these modules can be used to build an instrument suitable for microgravity research.

Crystallization of hard spheres, critical phenomena, nucleation, spinodal decomposition, gelation, aggregation, diffusion, etc. are influenced by gravity and can be studied more effectively with LLS in a reduced environment. A number of classic texts exist on LLS (photon correlation spectroscopy, PCS), see references 3, 4, 5, 6, 7, 8, 9, 10, 11, 12, 13, 14. LLS can enhance protein crystal growth experiments which need quantitative information about the growth process and an indication of the onset of nucleation. Dynamic light scattering is used for measuring and correlating fluctuations in the intensity of the light scattered from particles in Brownian motion. This gives a diffusion coefficient from which particle sizes in a range from 3 nanometers to above 3 microns are derived. Static light scattering is the measurement of the time-averaged intensity scattered by dispersions of particles and macromolecules (e.g. polymers, proteins, micelles, microemulsions, etc.) and is an important tool for the determination of particle structure, weight-averaged molecular weight and particle interactions. Dynamic depolarized laser light scattering examines the weak, horizontally-polarized light scattered from a sample illuminated by a vertically polarized laser beam and derives dynamic and structural information from this (e.g., rotational properties and particle aspect ratios), which is not otherwise readily available.

(a) Correlator Card

Brookhaven Instruments has developed a single board correlator (BI-9000AT) which has been designed and built to decouple the sampling times and the delay times and to have an absence of any prescaling requirements. It spans a time range of more than 10 decades by optimizing the hardware for 3 ranges: a group of fixed channels from 25 ns to 2.4 μs, a group of up to 256 channels from 0.5 to 100 μs and a group of up to 240 channels from 50 μs to 1310 sec. Channel spacing may be linear, constant ratio or user selected spacing. The correlator also has an onboard processor and numeric coprocessor which presently allows the independent operation of up to 8 of these cards simultaneously on a computer bus. This mode of operation is ideally suited for simultaneous multi-angle experiments or simply for redundancy in space flight experiments.

(b) APD Detector

The ideal PCS detector would have wide spectral sensitivity, 100% photon detection efficiency, zero dark count, zero afterpulsing, reignition or latching, zero deadtime, a linear count rate up to infinitely high count rates, zero timing jitter, a diameter perfectly matched to the application and room temperature operation. No such detector exists, and until recently the photomultiplier tube (PMT) has been the best compromise. Work at EG&G, partially funded by NASA Lewis and NASA Goddard, has led to a new generation of active quench circuits for geiger mode APDs (above the breakdown voltage, gains of 10^7 to 10^8), and a performance which comes closer to the ideal than has previously been available.

For a comprehensive review of recent work see reference 15. We note in passing that a helium cooled self-quenched VLPC detector (Visible Light Photon Counter) which is close to the ideal has been developed by Rockwell in collaboration with Fermi National Accelerator Laboratory.[16,17], and unpublished reports note useful subgeiger performance from nitrogen cooled high voltage APDs[18]. Neither of these however meet the requirements for compact room temperature operation in an inexpensive configuration.

Previous geiger mode commercial products, based on Slik™ APDs temperature stabilized on two stage thermoelectric coolers have been limited by passive quench circuitry to 'soft' RC recharge deadtimes of ~250ns at overvoltages of 5V to 7V. This gave peak photon detection efficiencies (P_d) values around 45% at 650nm over a <150 micron diameter, with typical dark counts as low as 40ct/s in regular production, and <1ct/s on a 'hero' detector.

A new active quench circuit being prepared for commercial introduction in mid-1994 operates the same detectors at overvoltages of around 25V to give a deadtime around 50ns and an active diameter around 300 microns (Figure 1). Deadtimes as low as 30ns has been observed with exceptional chips on breadboard layouts. The higher P_d of around 70% over their larger diameter leads to a typical dark count at minus 10°C on a two stage thermoelectric cooler of around 100 to 400 ct/s.

Figure 2 shows the autocorrelation function taken with the 25ns Brookhaven BI-9000AT correlator described in section (a). The deadtime is <50ns. Some afterpulsing is observed, related to residual detector impurities. The levels of both afterpulsing and dark count vary from chip to chip; typical range and selectable values remain to be established; Figure 3 shows an accurate measure of afterpulsing using a delayed coincidence technique. Total afterpulsing is around 0.12%. Figure 4 shows a linearity curve, where the 'Correction Factor' is the factor by which the observed count should be multiplied to give the corrected linear count. At count rates above ~10Mct/s, self-heating of the chip leads to additional non-linearity above that expected from dead-time alone. Though generally not relevant in PCS, an important feature of the circuit for Lidar applications is the ability to gate the overvoltage from overload levels and hence avoid the thermal recovery time constant over a few tens of seconds.

The hermetically sealed, thermoelectrically (TE) cooled detector, together with active quench circuit, output buffer, stabilized high voltage supply and TE cooler driver is incorporated in 132 x38x102 mm aluminum alloy module. It operates from a single 5V, 1.2A (max.) supply, outputs 50ohm TTL pulses, and gives stable performance over a module temperature range from 5°C to 40°C. An FC connectorized head is available for fiber coupled applications.

A nominally attractive alternative to geiger mode is photon counting with APDs at very high gain in the subgeiger mode (biased below breakdown), since afterpulsing, reignition, and latching will be zero. Count rates in excess of 10Mct/s and dead times below 50ns have been demonstrated, but at the expense of P_d below 15% and high dark counts (Ref. 19 and internal work at EG&G). The limiting factor has been breakdown and therefore gain non-uniformity over the APD surface, which prevents the achievement of the high uniform gains of close to one thousand required for useful P_d and low noise; to date this has been an intractable problem, though research continues.

(c) Laser Diodes

have

The pioneers for using both laser diodes[20] and APD detectors[21, 22, 23, 24, 25] for photon correlation spectroscopy were R.G.W. Brown and his research colleagues at Royal Signals and Radar Establishment (RSRE) in the U.K. Robert Brown's contributions to our group as a consultant ~~has~~ been a great asset to our program. We have used laser diodes in our laboratory for both laser light scattering and surface light scattering. We use both pigtailed laser diodes (available from SeaStar Optics, Inc.) and laser diodes with collimating lenses. Laser diodes suitable for photon correlation spectroscopy are available both in the visible and infrared and can be very inexpensive if they are not pigtailed. Diodes and their battery power supplies which can generate 3mW single mode CW light are typically only a few hundred dollars (US) each.

Voltage variation across the APD during the active quench and reset.

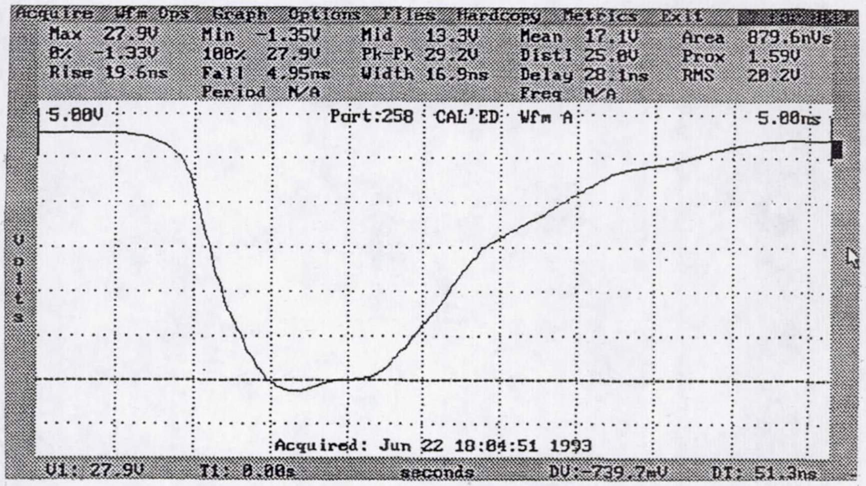

Figure 1a
5ns/div. (counting rate = 4,000,000 cps)

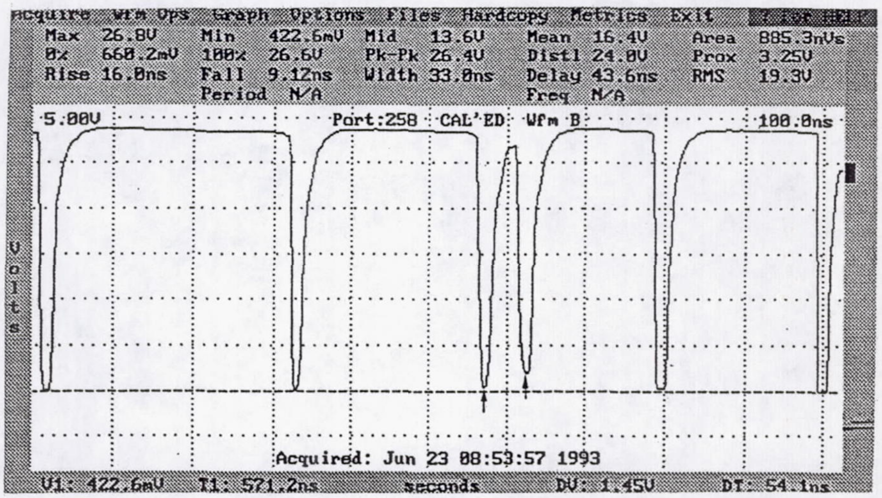

Figure 1b
100ns/div. (counting rate = 4,500,000 cps)

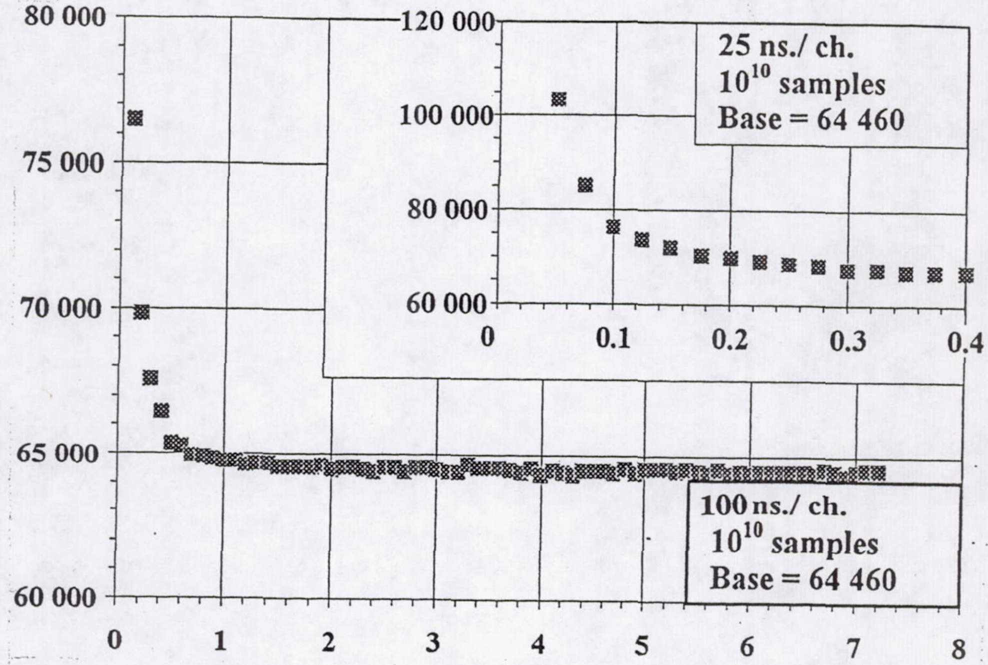

Figure 2a

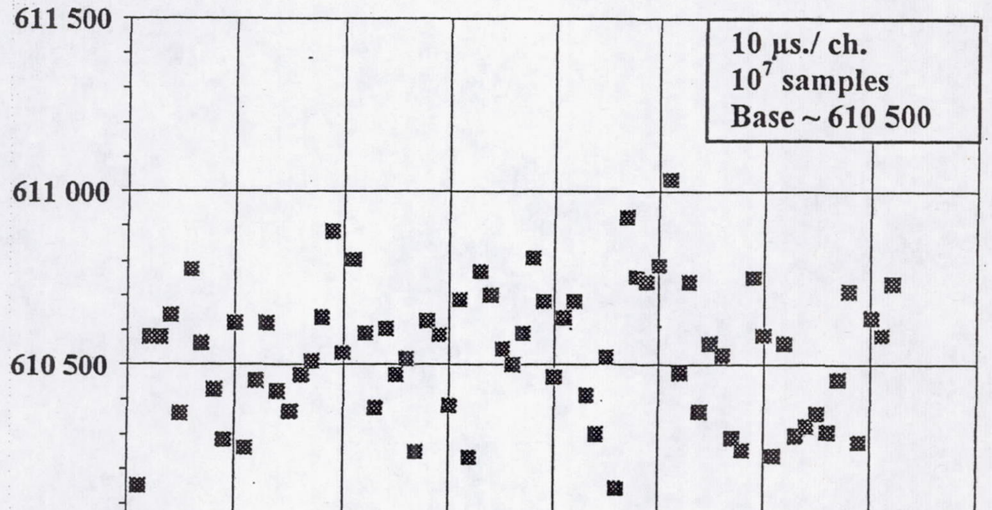

Figure 2b

Vertical scale: autocorrelation function,
Horizontal scale: time in microseconds.

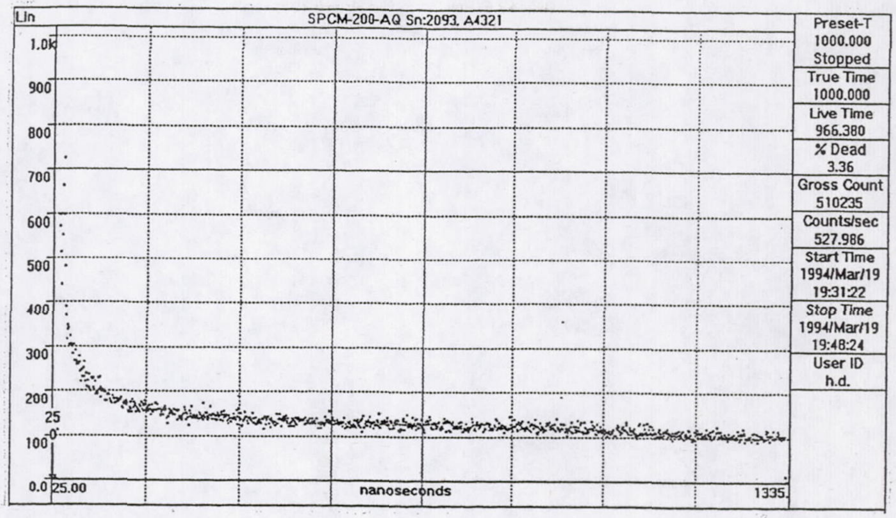

Figure 3

After-pulse Measurements
If one removes the slow decay component due to chance events (exponential decay corresponding to a Poisson distribution) one obtains a value of ~0.125% for the after-pulse probability.

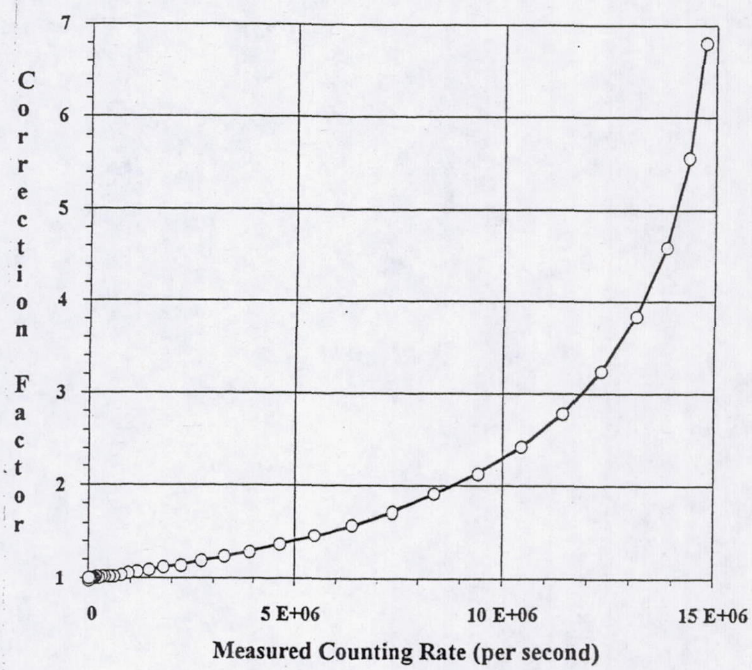

Figure 4

Linearity SPCM-200-AQ, SN:2093
The correction factor corresponds to the ratio of incoming photons over detected photons (not taking into account the photon detection probability which is constant).

(d) Fiber Optics

We have chosen to use fiber optic cables for source and detection paths to minimize alignment problems. By selecting FC/PC connectors we have a self-aligning connector which is polarization preserving and reliable. This connector uses a ceramic insert housed in a stainless steel body to hold and align the fiber, and when disconnected emits a diverging cone of light since it does not contain an integrated lens. This helps us address safety concerns.

Significant advances in fiber optic probes[26,27] and backscatter probes[28] have been used by and initiated by NASA's LLS ATD project with Professor H.S. Dhadwal at SUNY-Stony Brook. One version of the fiber optic probes allows LLS to be used in a solution that does not allow a laser beam to pass through it without multiple scattering. The study of milky concentrations of polystyrene standards in water ranging up to 10% weight concentration without multiple scattering problems was enabled through the use of these backscatter probes.[29] Work with high concentration protein solutions without the multiple scattering problems was successfully accomplished by using LLS and backscatter fiber optic probes. The probes have proved to be of great importance when LLS is applied to protein crystal growth experiments[30]. Reference 30 discusses the detection of the size of BSA and Lysozyme proteins in solutions of varying concentration. Reference 31 discusses how the idea of determining protein crystal size can be coupled with the miniature (pencil-sized), lensless backscatter fiber optic probe to study and monitor cataract development. When the protein aggregates in the eye lens grow large enough, they are referred to as a cataract. To be able to monitor this process before and while it is advancing will provide an invaluable diagnostic tool. Additionally, microemulsions were also successfully characterized with improved results using the noninvasive probe.[32]

We have also successfully looked at protein crystals by a fiber optics beam delivery and receiving system using with a ninety degree scattering cell and a pair of GrIn (Graded Index) lenses. These lenses can be either butt-coupled to FC/PC connectors or attached with UV curable epoxies directly to the fibers. This is most easily done by launching a laser beam into a fiber using a microscope objective (~ x20) and a laser of the appropriate wavelength. When cementing the cleaved fibers and GrIn lenses, the other end of the fiber is held in a Newport ULTRAlign™ chuck which is placed next to a 3-axis Newport ULTRAlign™ positioner. A small amount UV curable epoxy (available from Norland) is applied after the fiber is appropriately position at the center of a 0.25 pitch GrIn lens. When a nice Gaussian beam is observed on the wall several meters away, a UV gun is used to cure the epoxy. Extremely small GrIn lenses produce diffraction rings rather than a Gaussian profile. We have used this technique with lenses ranging in diameters from 300 microns (which is challenging, see Figure 5) to several mm.

(e) CDOT Glovebox Experiment

Aspects of all the preceding components have been utilized in the Colloidal Disorder-Order Transition (CDOT) glovebox experiment which is manifested on the next US Microgravity Laboratory space shuttle mission (USML-2) currently scheduled to launch in September 1995. The space shuttle glovebox is a facility that provides an interactive, contained environment for small microgravity experiments (the working volume is approximately 400 x 280 x 230 mm). The CDOT instrument will be used to characterize the phase transitions of a hard sphere system in a microgravity environment. CDOT will measure the temporal autocorrelation function of scattering intensity at 90 degrees (dynamic light scattering) and the static light scattering intensity as a function of scattering angle (Bragg scattering). This data will allow us to characterize the structure and rheology of the colloidal system under investigation as a function of particle concentration.

CDOT is the first of two space shuttle experiments currently funded to investigate hard sphere interactions. The second experiment, Physics of Hard Spheres Experiment (PH^{A}SE), will make high resolution Bragg scattering measurements, observe the onset of nucleation and growth, and accommodate multiangle dynamic light scattering. CDOT will serve as a pathfinder experiment for PH^{A}SE while providing the initial data set on the characteristics of a hard sphere system in microgravity. The CDOT

SOMEWHERE PUT STANDARD NASA DISCLAIMER: eg not recommending particular instruments etc.

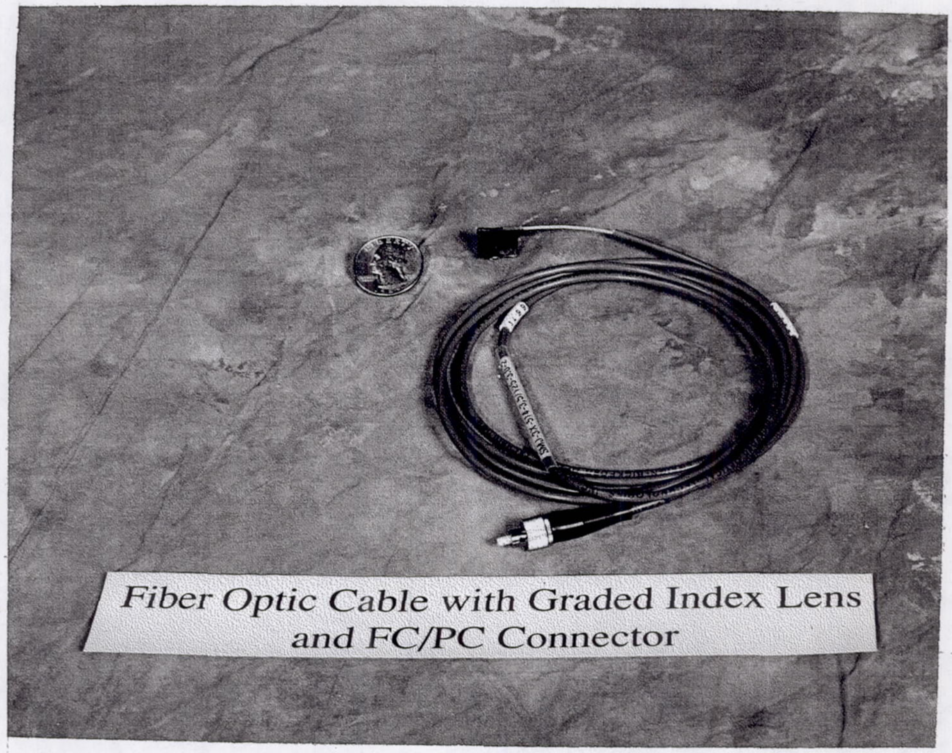

Figure 5

experiment hardware consists of sample cells, an experiment module, a power/controls box, experiment cabling, and a laptop computer (Figure 6).

We will observe 0.5μm diameter Poly(Methyl Methacrylate) (PMMA) spheres suspended in a mixture of decalin and tetralin. The index of refraction of the solvent mixture is closely matched to that of the PMMA particles (n~1.5). The samples will be contained in 10 mm OD (8 mm ID) x 120mm cylindrical fused silica cells. 16 samples will be flown with hard sphere volume fractions ranging from .49 to .58. An astronaut will homogenize the samples on orbit and then allow them to sit undisturbed for approximately 5 days while the samples reach equilibrium. The astronaut will then place the samples one by one into the experiment module for observation.

The experiment module consists of the laser source, photodetector, experiment optics, and sample cell stage with translation and oscillation motors (Figure 7). It measures 207 x 189 x 206 mm and weighs approximately 5.5kg. One of the most innovative features of the experiment module is the consolidation of the laser source and the photodetector into a single, compact module developed by EG&G. The laser source in our engineering model (EM) unit is a 30mW, 780nm laser diode (Sharp #LT025MDO) pigtailed to an FC connector and thermally controlled with a Peltier cooler. The flight hardware will use a 670nm laser diode (e.g. Toshiba TOLD 9150) for easier detection by the human eye during ground testing and verification. The photodetector is the EG&G active quench/active reset APD described in section (b). The laser and the APD share a 5V power source (4A max., 2.5A typical), and the module is passively cooled. The source/detector module measures 48 x 150 x 153 mm and weighs less than 1kg.

Two polarization preserving, single mode optical fibers terminated with FC/PC connectors link the source/detector module with the experiment test section. The launching fiber delivers the laser beam into a lens which focuses the exiting laser light into a 50μm diameter beam through the center of the sample cell and into a beam stop below the cell. The polarization of the laser is along the axis of the sample cell.

Figure 6

The sample cell focuses light having the same scattering angle to a ring 15mm from the center of the cell. The pickup fiber is a single mode fiber located 15mm from the center of the cell and oriented perpendicular to the launching fiber to pick up the light scattered at 90 degrees (Figure 8). The core of the fiber is so small that it only picks up one speckle spot. The fluctuating signal is fed into the APD and the temporal autocorrelation function is measured with the BI-9000AT digital correlator described in section (a).

We use the temporal autocorrelation function to study the dynamics of colloidal particles in an ordered state. In a crystal state, the colloidal particles undergo random Brownian motion due to their thermal collisions with the solvent molecules. The motion of particles is restricted around their lattice positions because of the interactions between the particles, and the maximum mean square displacement is less than that set by the Lindemann criterion, which defines the melting condition. Coherent light scattered by a colloidal crystal is a superposition of two parts. The first part is a fluctuating intensity due to the motion of the particles around their lattice sites. The second is a fixed speckle pattern arising from the time-invariant fixed crystal structure. The ensemble-averaged temporal autocorrelation function of scattered light probes the motion of particles. To measure the ensemble-averaged temporal autocorrelation function, we fix the detector position and slowly translate the sample. We do this using a linear translation motor to drive the sample stage and employ Hall effect sensors to control the limits of the motor travel. As the sample translates, the speckle pattern changes at the detector position. This way, we obtain the ensemble-averaged temporal autocorrelation function.

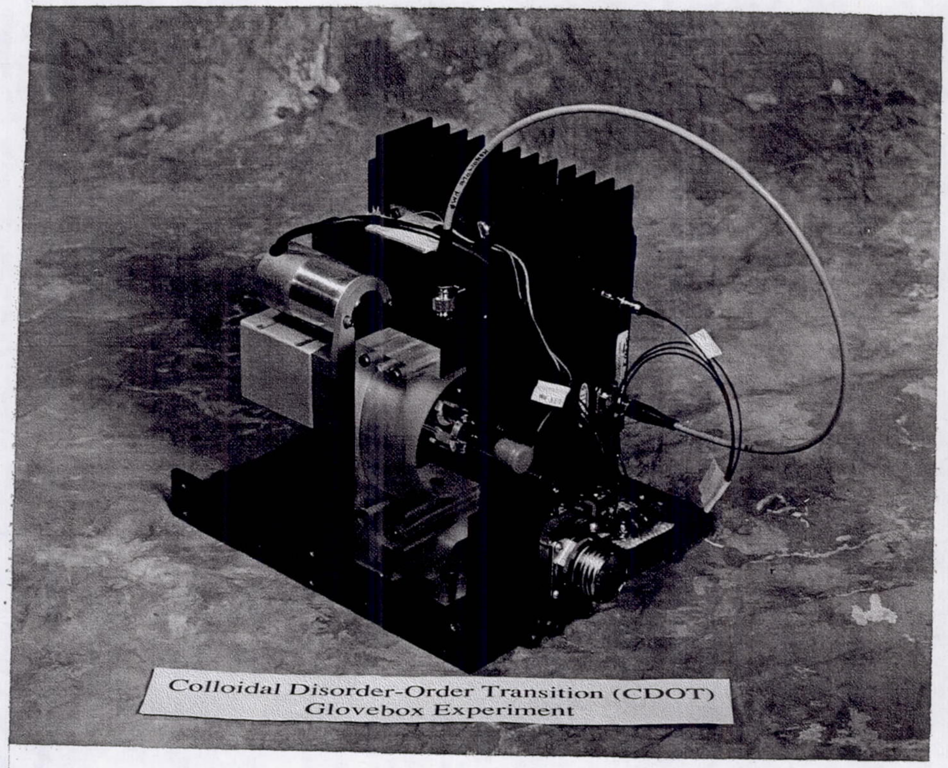

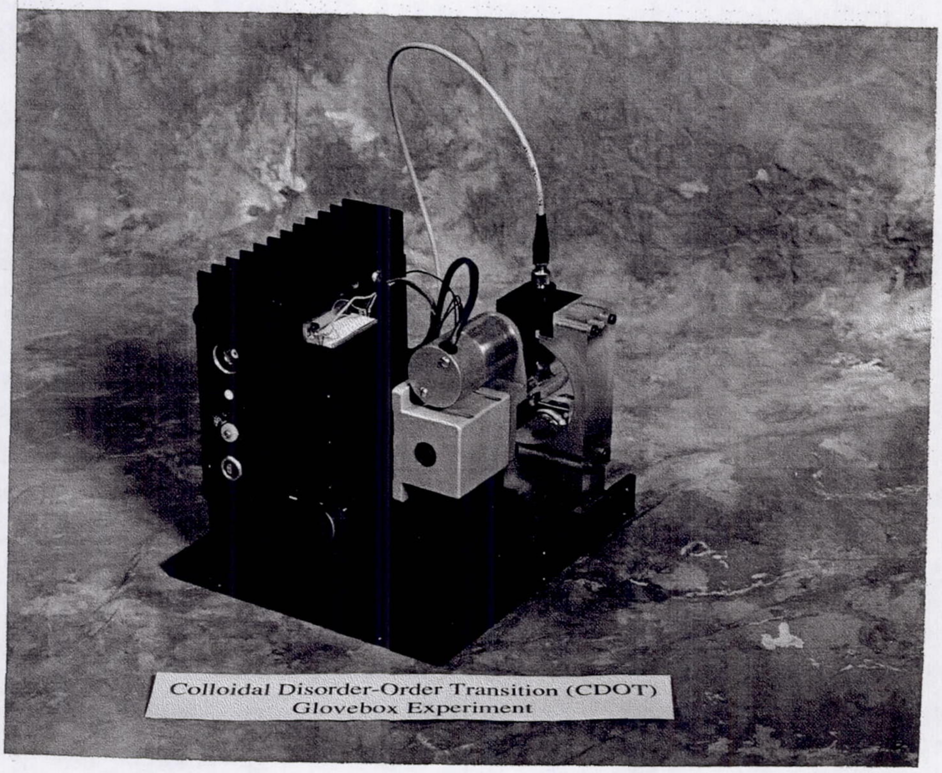

Figure 7
CDOT Glovebox Module
Front view at top of page
Back view at bottom of page

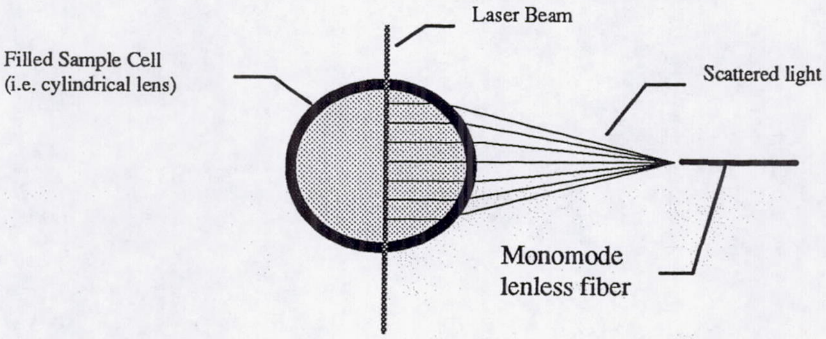

Figure 8

On the opposite side of the receiving fiber, we use a 20mm diameter cylindrical lens concentric with the sample cell to focus light with the same scattering angle to a ring with a radius of 30mm concentric with the axis of the sample cell. To detect the intensity at any scattering angle, we use a CCD camera to record the images formed on a 30mm cylindrical diffuse screen placed at the ring as the linear translation motor moves the sample back and forth beneath the laser beam. Post-flight, we will digitize the images with a frame-grabber and produce a time-averaged composite to obtain the intensity as a function of angle. The location of the Bragg rings produced by this method will indicate the type of structure in the crystallized samples (an FCC crystal is predicted).

We obtain the shear modulus of colloidal crystals by measuring the amplitude of oscillations as a function of frequency. A DC motor on the CDOT experiment module is outfitted with an eccentric hub on its shaft which drives the sample cell collet assembly back and forth in a 2° arc about the axis of the cell with a variable frequency. This applies an oscillatory external shear force to the colloidal crystal within the cell and produces a strain, S. The recovery force is then the product of the shear modulus, G, and the strain. For a colloidal crystal in an infinite cylindrical cell, the amplitude is given by

$$A(\omega) = \frac{J_1\left(\sqrt{\frac{\rho\omega^2}{G' + i\omega\eta}}\,r\right)}{J_1\left(\sqrt{\frac{\rho\omega^2}{G' + i\omega\eta}}\,R\right)} A_0 \sin\omega t$$

where ω is the frequency, R the radius of the sample cell, r the radial distance from the center of the cell, and A_0 the amplitude at the boundary of the cell. Here we also assume that the viscosity is so small that it can be ignored, $\eta \ll \frac{G'}{\omega}$. The amplitude of the oscillation goes to infinity as $J_1\left(\frac{\omega}{\sqrt{\frac{G}{\rho}}}R\right)$ goes to zero. The first root for J_1 is 3.81. It is clear from the above equation that the first resonant frequency is at $\omega = 3.81\sqrt{\frac{G}{\rho R^2}}$. Therefore, we can obtain the shear modulus by experimentally determining the resonance frequency.

The glovebox facility provides 12V and 24V power to the experiment via the CDOT power/controls box, which is located outside the glovebox. The 12V power is used to operate the translation and oscillation motors, and the 24V power is stepped down to 5V for the source/detector module. The power/controls box provides both transient and overcurrent protection and contains a portion of the control electronics for the motors. The remaining motor control electronics reside on a Quatech SAC-12 motor controller card in the shuttle laptop computer.

A unique feature has been implemented in the design of the CDOT power, signal, and experiment data cabling for the microgravity environment. In reduced gravity, cables tend to behave rather unpredictably and can end up interfering with mechanical assemblies, drifting into camera views, or even moving hardware around when the experiment is small (like a glovebox experiment). To prevent such problems, a length of solid copper 14 AWG wire will be run in each leg of the cabling. This will allow the astronaut to mold the cable into a desired shape and will help the cable retain that shape throughout the course of the experiment.

The entire experiment sequence including correlator functions, translation, and oscillation will be controlled from one of the shuttle payload general support computers outfitted with an expansion box containing the BI-9000AT correlator card and the SAC-12 motor controller card. The experiment software will utilize control scripts making the experiment highly automated.

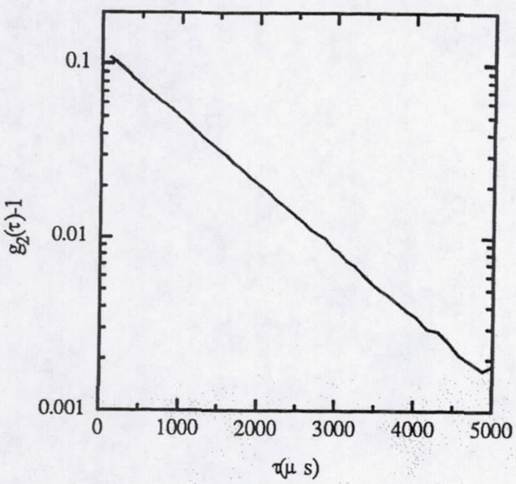

Figure 9

To test the CDOT hardware, we measured the autocorrelation function of light scattered from a dilute solution (about 10^{-3} to 10^{-4} volume fraction) of monodisperse, standard-sized polystyrene spheres in water. The diameter of the polystyrene spheres (from Duke Scientific) was 0.222μm with a standard deviation of 1.7%. The temporal autocorrelation function is plotted semi-logarithmic in Figure 9. As we expected, the autocorrelation function decays exponentially as a function of delay time. The slope of the decay gives a diffusion coefficient of 1.9×10^{-8} cm^2/s. Using the Einstein-Stokes formula, we obtain the diameter of 0.223μm, as we expected. This measurement indicates that our design of the CDOT experiment enables us to accurately measure the temporal autocorrelation function at 90 degrees.

Summary

We have reviewed recent laser light scattering hardware advancements which were used by or developed for a NASA Advanced Technology Development program. The advancements include a digital correlator reduced to a single board, an active quench/active reset APD which has been combined with a laser diode to form a compact laser source/detector module, and a number of fiber optic applications. The CDOT glovebox experiment demonstrates how these advancements can be used to build rugged, compact microgravity experiments with enhanced capabilities.

Acknowledgments

Five of the authors (WVM, PT, RBR, RRA, JZ) would like to thank Code UG (Microgravity Science and Applications Division) at NASA Headquarters for its support. WVM and RRA would like to recognize the encouragement and support of T.K. Glasgow who, as a branch chief at NASA Lewis, helped see the Advanced Technology Development program in laser light scattering through its youth.

The EG&G authors wish to particularly thank Bill Meyer of NASA Lewis and James Spinhine of NASA Goddard for their patient support and encouragement of this work.

The NASA Lewis authors would like to thank Mario Romanin, Allen Rybar, Joseph Tammaro, Janice Duke and the rest of the design team at ADF, the staff of the fabrication shop at NASA Lewis, and Brian Quigley who manages all of the glovebox experiments at NASA Lewis.

Paul Chaikin and Bill Russel at Princeton have been the scientific mentors for the CDOT glovebox experiment. They proposed the original scientific goals which were peer reviewed and deemed worthy of flight. The NASA Lewis authors and JZ would like to thank them for their encouragement, support, and overall direction of the scientific goals in the project. This work is an integral part of the development of the $PH^{A}SE$ flight hardware which is being designed with additional direction from David Cannell (University of California - Santa Barbara), David Weitz (Exxon), John Abbiss and Anthony Smart (Titan/Spectron), and the NASA Lewis $PH^{A}SE$ team.

References

[1] "Proceedings NASA Laser Light Scattering Advanced Technology Development Workshop, 1988", CP10033, published August 1989, edited by W.V. Meyer.

[2] Meyer, W.V. and Ansari, R.R. , "A Preview of a Microgravity Laser Light Scattering Instrument", AIAA 91-0779. This paper was presented January 9, 1991 at the 29th Aerospace Sciences Meeting.

[3] Barth, H. G., editor, "Modern Methods of Particle Size Analysis," Chapter 3 - Particle Sizing Using Photon Correlation Spectroscopy, Weiner, Bruce B., John Wiley & Sons, NY, 1984.

[4] Berne, B. J., Pecora, R., "Dynamic Light Scattering," John Wiley & Sons, NY, 1976.

[5] Bohren, C. F., Huffman, D. R., "Absorption and Scattering of Light by Small Particles," John Wiley & Sons, NY, 1983.

[6] Chu, B., "Laser Light Scattering," Academic Press, NY, 1974.

[7] Chu, B., editor, "Selected Papers on Quasielastic Light Scattering by Macromolecular, Supramolecular, and Fluid Systems," SPIE Milestone Series, Volume MS 12, SPIE Optical Engineering Press, Bellingham, Washington, 1990.

[8] Cummins, H. Z., Pike, E. R., editors, "Photon Correlation and Light Beating Spectroscopy," Plenum Press, NY, 1973.

[9] Cummins, H. Z., Pike, E. R., editors, "Photon Correlation Spectroscopy and Velocimetry," Plenum Press, NY, 1977.

[10] Dahneke, B. E., "Measurement of Suspended Particles by Quasi-Elastic Light Scattering," John Wiley & Sons, NY, 1983.

[11] Degiorgo V., Corti, M., Giglio, M., editors, "Light Scattering in Liquids and Macromolecular Solutions," Plenum Press, NY, 1979.

[12] Kerker, M., "The Scattering of Light and Other Electromagnetic Radiation," Academic Press, Inc., Orlando, 1969.

[13] Pecora, R., editor, "Dynamic Light Scattering, Applications of Photon Correlation Spectroscopy," Plenum Press, NY, 1985.

[14] van de Hulst, H. C., "Light Scattering by Small Particles," Dover Publications, Inc., 1957.

[15] H. Dautet, Pierre Deschamps, Bruno Dion, Andrew D. MacGregor, Darleene MacSween, Robert J. McIntyre, Claude Trottier, and Paul P. Webb, "Photon counting techniques with silicon avalanche photodiodes," Applied Optics, 32, 21, 3894-3900 (1993).

[16] M. D. Petroff and M.G. Stapelbrock, IEEE Transactions on Nuclear Science, Vol. 36, No. 1, (1989), pp 158-162.

[17] M. D. Petroff and M. Atac, IEEE Transactions on Nuclear Science, Vol. 36, No. 1, (1989), pp 163-164.

[18] N.G. Woodward, et al., "Photon Counting Using a Large Area Avalanche Photodiode Cooled to 100K," Dept. of Physics, Ohio State University, private communication.

[19] X. Sun and F.M. Davidson, "Photon counting with silicon avalanche photodiodes," J. Lightwave Technol., 10, 1023-1032 (1992).

[20] Brown, R. G. W. and Grant, R., "Photon Statistical Properties of Visible Laser Diodes," Rev. Sci. Instrum. 58 928-931, 1987.

[21] Brown, R. G. W., Ridley, K. D., Rarity, J. G., "Characterization of Silicon Avalanche Photodiodes for Photon Correlation Measurements, 1, Passive Quenching," Appl. Opt. 25, 4122-4126, 1986.

[22] Brown, R. G. W., Jones, R., Ridley, K. D., Rarity, J. G., "Characterization of Silicon Avalanche Photodiodes for Photon Correlation Measurements, 2, Active Quenching," Appl. Opt. 26, 2383-2389, 1987.

[23] Brown, R. G. W., Daniels, M., "Characterization of Silicon Avalanche Photodiodes for Photon Correlation Measurements, 3, Sub-Geiger Operation," Appl. Opt. 28, 4616-4621, 1989.

[24] Brown, R. G. W., "Miniature Instrumentation for Laser Light Scattering Experiments," from NASA Laser Light Scattering Advanced Technology Development Workshop--1988, NASA Conference Publication 10033, 45-64.

[25] Brown, R. G. W., Burnett, J. G., Mansbridge, J., Moir, C. I., "Miniature Laser Light Scattering Instrumentation for Particle Size Analysis," Appl. Opt. 29, 4159-4169, 1990

[26] MacFadyen, A. J., Jennings, B. R., "Fibre-Optic Systems for Dynamic Light Scattering -- A Review," Optics & Laser Technology, **22 No. 3**, 1990.

[27] Dhadwal, H.S., Khan, R.R., Suh, K., "An Integrated Fiber Optic Probe for Dynamic Light Scattering", J. App. Optics, Vol. 32, No. 21, July 20, 1993.

[28] Dhadwal, H.S., "A Back Scatter Fiber Optic Probe For Particle Sizing", Gradient-Index Optical Systems Topical Meeting, Topical Meeting, Monterey, CA. April 8-9, (1991).

[29] Dhadwal, H.S., Ansari, R.R., and Meyer, W.V., "A Fiber Optic Probe for Particle Sizing in Concentrated Suspensions", Review of Scientific Instruments 62 (12), December 1991.

[30] Dhadwal, H.S., Wilson, R.R., Ansari, R.R., and Meyer, W.V., "Dynamic Light Scattering Studies of BSA and Lysozyme using a Backscatter Fiber Optic System", Proceedings of Static and Dynamic

Light Scattering in Medicine and Biology, Biomedical Optics '93, 16-23, January 21-22, 1993, Los Angeles, CA.

31 Dhadwal, H.S. and Ansari, R.R., "A Coherent Fiber Optic Sensor for Early Detection of Cataractogenesis in a Human Eye Lens", J. Optical Engineering, Vol. 32, No. 2, pp 233-238, February 1993.

32 Ansari, R.R., Dhadwal, H.S., Cheung, H. M., and Meyer, W.V., "Microemulsion Characterization Using a Fiber Optic Probe", J. App. Optics, Vol. 32, No. 21, July 20, 1993.